

# Study of Aero-thermal Effects with Heat Radiation in Optical Side Window

Chun-Chi Li, Da-Wei Huang, Yin-Chia Su and Liang-Chih Tasi

**Abstract**—In hypersonic environments, the aerothermal effect makes it difficult for the optical side windows of optical guided missiles to withstand high heat. This produces cracking or breaking, resulting in an inability to function. This study used computational fluid mechanics to investigate the external cooling jet conditions of optical side windows. The turbulent models  $k-\epsilon$  and  $k-\omega$  were simulated. To be in better accord with actual aerothermal environments, a thermal radiation model was added to examine suitable amounts of external coolants and the optical window problems of aero-thermodynamics. The simulation results indicate that when there are no external cooling jets, because airflow on the optical window and the tail groove produce vortices, the temperatures in these two locations reach a peak of approximately 1600 K. When the external cooling jets worked at 0.15 kg/s, the surface temperature of the optical windows dropped to approximately 280 K. When adding thermal radiation conditions, because heat flux dissipation was faster, the surface temperature of the optical windows fell from 280 K to approximately 260 K. The difference in influence of the different turbulence models  $k-\epsilon$  and  $k-\omega$  on optical window surface temperature was not significant.

**Keywords**—aero-optical side window, aerothermal effect, cooling, hypersonic flow

## I. INTRODUCTION

RESEARCH into aero-optics includes probes by high-speed flow on onboard imaging, the influence of atmospheric turbulence on optical images, and their corrections. This method is primarily applied to the new generation of interceptor missiles, the hood sides of which are called optical hoods. In general, these hoods are composed of three sections: casings, optical windows, and optical window cooling systems. The nearby optical windows receive infrared rays to guide tracking and intercepting high-speed aircraft. When interceptor missiles are flying at high speeds in the atmosphere, complex flow fields form between their optical windows and the airflow. This results in high heat, thermal radiation, and interference with image transmission in the seeker, leading to target image offsets, jitter, and fuzziness. This is called the aero-optical effect. The aero-optical effect includes the high-speed flow field optical transmission effect, shock waves, the window aerothermal radiation effect, and the optical window aerodynamic heating effect, as shown in Fig. 1. [1]

C. C. Li is with the Department of Mechatronic, Energy and Aerospace Engineering, Chung Cheng Institute of Technology, National Defense University, Taiwan, ROC (corresponding author to provide phone: 886-3-3803043; fax: 886-3-3895924; e-mail: davidli560607@gmail.com).

D. W. Huang & Y. C. Su are with the School of National Defense Science Studies, Chung Cheng Institute of Technology, National Defense University, Taiwan, ROC (e-mail: syc6717@gmail.com).

L. C. Tasi is with the Master program Mechanical Engineering, Chung Cheng Institute of Technology, National Defense University, Taiwan, ROC (e-mail: aeroflightalex@gmail.com).

The high temperatures produced by the aerothermal effect result in heat loads, cracks, failure, and even rupture in the optical windows, influencing the normal operation of optical detection systems. In general, cooling technology must be used for protection and for lowering temperatures. Two methods are primarily adopted for optical window cooling, external jet cooling and internal convection cooling. This study investigates the aerothermal effect of external jet cooling. In external jet cooling, low-temperature airflow is sprayed from the front of the window (or all around it) on the outside of the window, forming a membrane and separating the optical window from the external hot airflow, thus providing insulation and cooling for the window. This demands that a uniform, stable gas membrane forms on the outside of the window during the entire work process. This method is also called external jet film cooling. The external cooling method is simple and easy to implement, but cooling gas and the gas boundary layer mix, forming a shear/mixed layer. Thus, complex turbulence flow fields and the aero-optical effect easily occur.

Currently, two forms for optical windows exist. The first is a mosaic window, which has a superior line of sight and tracking range, and does not require external aircraft roll control systems for alignment. However, the substantial optical diffraction effect, low aperture efficiency, and complex structure and processes are difficulties that must be overcome. The second type is the side-cooled optical window. In general, a planar optical window is installed on the surface of the side of the hood region. The position of the window is slightly lower than the missile surface maintaining the hood's appearance. The beams are not restricted by the optical window aperture diffraction limit, and are easy to install. However, the most significant problem yet to be solved is that a large area of the optical window is exposed to the extremely hot boundary layer. When flying in the atmosphere, the optical window must be cooled.

Li et al. [2] simulated Terminal High Altitude Area Defense (TAAD) missiles at angles of attack from  $0^\circ$  to  $30^\circ$ . The turbulence method used was the Spalart-Allmar (SA) model. At a flying altitude of 30 km with a flight speed  $M = 6$ , by using active external cooling jet controls, when cooling air mass flow reached 0.15 kg/s, the entire optical window could be cooled to 500 K or less, protecting the function of the optical window. However, this study did not include thermal radiation conditions. Cooling jet may be over-forecast, leading to missile payload problems. In the study described above, the simpler SA turbulent model was adopted, and the problems of thermal radiation were not investigated. The actual optical transmission effect was caused by turbulence flow fields. The movement of turbulence flow fields was random and without rules, and there is yet no complete theoretical description of their laws of motion. This has been a hot topic in the field of fluid mechanics, and discussion of which turbulence model is most applicable to the aerothermal of aero-optical hoods remains inconclusive.

Bertin et al. [3] indicated that during hypersonic flight at altitudes of 30 to 50 km, the aerothermal effect impacted the reliability of the material structure of optical windows, forcing the installation of a temperature protection system (TPS) on the flying body. Neale and Max [4] divided TPS conceptually into passive, semi-passive, and active models, as shown in Fig. 2. However, because the introduced cooling jets produce more complex mixed shearing phenomena with the mainstream, the chaotic features of the flow field are further intensified, influencing the interpretation of images by the infrared system within the optical window. Thus, calculating aero-optical influence quantitatively and adopting effective methods for calibration is a key issue in the development of high-speed interceptors. Hirschel [5] indicated that at altitudes of 50 km and less, the flow fields of flying bodies were governed by the viscous effect. The wall heat radiation effect must not be overlooked. Therefore, in actual conditions, the influence on temperature brought by the aerothermal radiation effect and the interfering noise of thermal radiation must be considered. In actual situations, the emissivity, absorption rate, index of refraction, and reflectivity of a material are functions of temperature and wavelength. Bartl et al. [6] indicated that the emissivity of opaque aluminum materials decreased following increases in radiation wavelength, whereas reflectivity increased. Similarly, semitransparent materials, such as sapphire crystals, showed different optical properties under changing environmental temperatures and radiation wavelengths. Dobrovinskaya et al. [7] indicated that the emissivity, reflectivity, absorption rate, and penetration of sapphire all change following changes in incident wavelength.

Following Li's research on external cooling jets for optical side windows, this study adds two different turbulence models,  $k-\varepsilon$  and  $k-\omega$ . In addition, a thermal radiation model was included to better conform to actual aerothermal environments and to investigate suitable amounts of external coolant and the aerothermal problems of optical windows.

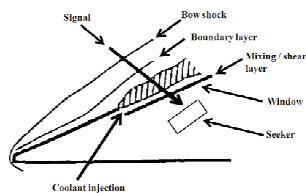


Fig. 1 Schematic diagram of aero-optical effects [1]

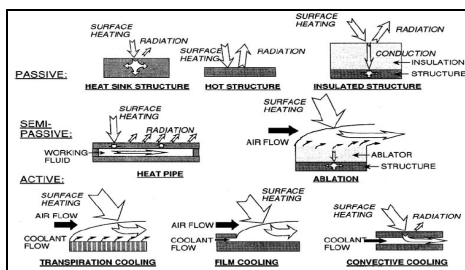


Fig. 2 Diagram of external cooling in different pattern [3]

## II. PROBLEMS AND METHODS

### A. Governing Equation and Numerical Methods

The governing equations are the Reynolds averaged Navier-Stokes equations, the conservation can be expressed as follows

$$\frac{\partial U}{\partial t} + \frac{\partial F}{\partial x} + \frac{\partial G}{\partial y} + \frac{\partial H}{\partial z} = \frac{\partial F_v}{\partial x} + \frac{\partial G_v}{\partial y} + \frac{\partial H_v}{\partial z} \quad (1)$$

In solving equation (1), convection terms ( $F, G, H$ ) are calculated by AUSM<sup>+</sup> scheme, while viscosity and diffusion flux terms ( $F_v, G_v, H_v$ ) are calculated using the central difference method. Discrete space terms are to form a group of ordinary differential equations followed by time integration to obtain the numerical solution.

### B. Turbulent and Radiation Models

In this paper, two different turbulence models adopted, including the realizable  $k-\varepsilon$  and standard  $k-\omega$  model. The majority of wave bands considered for use in heat-seeking missiles were infrared bands, with radiation wavelengths between 3 and 5  $\mu\text{m}$ . In addition, the research model in consideration investigated the optical transport phenomena of radiation absorption, penetration, refraction, reflection, and diffusion in opaque projectiles and semitransparent optical window materials. Thus, the non-gray discrete ordinate radiation model was used for simulation, with the radiative transfer equation provided below.

$$\nabla \cdot (I_\lambda(\vec{r}, \vec{s})\vec{s}) + (a_\lambda + \sigma_\lambda)I_\lambda(\vec{r}, \vec{s}) = a_\lambda n^2 I_{b\lambda} + \frac{\sigma_\lambda}{4\pi} \int_{\Omega} I_\lambda(\vec{r}, \vec{s}') \Phi(\vec{s} \cdot \vec{s}') d\Omega \quad (2)$$

### C. Boundary Conditions

This paper adopts computational fluid dynamics to study the external cooling characteristics of optical side window under different jet flow rates with flight speed of Mach 6, and 30 to 40 km altitude above sea level. The ambient pressure and ambient temperature are 50,000 Pa and 300K, respectively. The condition of inlet boundary and outlet boundary should be set at pressure-far-field condition and pressure-outlet condition, respectively. Besides, the cooling jet port is set to mass flow rates conditions. The projectile and optical window is set to no-slip and radiation conditions. Additionally, the real gas equation modified specific heat ratio is added.

### D. 3-D Physical Model and Grid Configuration

This paper assumes the optical window to be rectangular for ease of modeling and prediction of flow field. According to the observation, it is known that the cooling jet hole is located at the bottom of leeward and its size is approximately half the height of leeward. Besides, the former configuration shows a groove tilt with a deep front and shallow end. Schematic model of missile is shown in Fig. 3. Adopted in this study three-dimensional computational grid of structural grid configuration shown in Fig. 4, for the confirmation of the computational grid is independent of the characteristics of the grid, for 300,000, 500,000 and 800,000 three kinds of fine mesh window in the same flow conditions (cooling jet = 0.15kg/s) test. The test results on the optical window position

(0.11~0.3m) of the surface temperature are shown in Fig. 5. 500,000 and 800,000 in the optical window grid has a more consistent temperature performance, and ultimately the results will be 500,000 of total grid as a follow-up study.

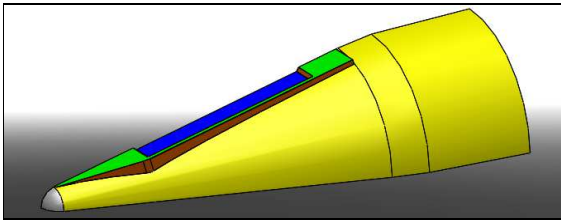


Fig. 3 THAAD guidance section model diagram

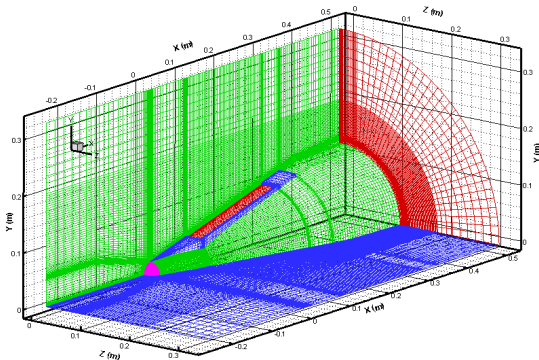


Fig. 4 3-D THAAD optical window grid diagram

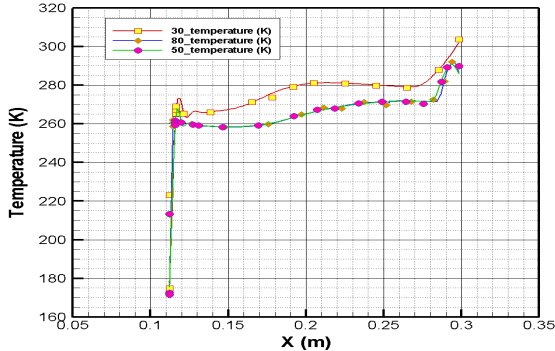


Fig. 5 Surface temperature of optical window in 3 type grid system

III. RESEARCH MATRIX

The different turbulent models are named Model A, B. The external cooling jet flow is divided into 2 categories according to their spray flow rates (J) including 0 (kg/s) and 0.15 (kg/s). Table 1 indicates the research matrix.

TABLE I  
RESEARCH MATRIX

Jet Flow(kg/s)	J=0	J=0.15	J=0.15& (radiation)
k-ε	A_0	A_1	A_2
k-ω	B_0	B_1	B_2

IV. RESULTS AND DISCUSSION

A. Numerical Code Validation

To verify the correctness of the formula in this software, the

numerical simulation results of hypersonic flow passing through a ramp channel obtained by Algacyr Jr. [8] were referenced for comparison. The operating conditions included an inviscid flow, a Mach number of 3.5, an environmental temperature of 300 K, and a pressure of one atmosphere for two-dimensional flow field simulation. The isobaric charts for the simulation results are shown in Figs. 6 and 7. Comparison of the isobaric line distribution indicated that angles of the oblique shock waves, characteristics of the expansion waves, and the position and angle of the reflected wave on the wall were all extremely similar. The expected high-speed flow field characteristics were captured correctly, indicating that the simulation software used in this study can be feasibly applied to high-speed flow fields.

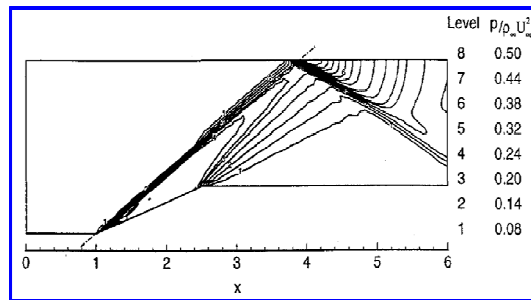


Fig. 6 Numerical simulation of Algacyr Jr. [8]

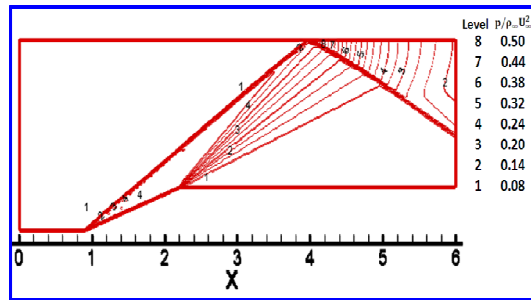


Fig. 7 Numerical simulation of present study

B. Optical Side Window Simulation Results

First, optical hoods flying at Mach 6 were simulated in conditions without cooling jets and without considering thermal radiation conditions. The results indicated that the surface temperature of the optical window was between approximately 1550 and 1620 K. Hot airflow on the optical window and the tail groove formed vortices, thus temperatures were higher. The optical window surface temperatures of the two turbulent models did not differ much, as shown in Figs. 8 and 9. The surface temperatures of the optical windows all exceeded the upper limit heat resistance temperature of 500 K in sapphire optical windows. Therefore, cooling jets had to be used.

When jet cooling was performed on optical side windows, the high-speed mainstreams that were initially close to the optical window surface were lifted upward due to injection of the cooling jets. In situations where the speeds of the jets and the mainstreams differed, the two produced a clear shear layer, as

shown in Fig. 10~11. In conditions with cooling jets, when no thermal radiation was observed as shown in Fig. 10, the surface temperature of the optical windows dropped to approximately 280 K. Outside of the optical window, with no cooling jets, the hood nose and the surrounding area maintained a high temperature of approximately 1500 K. Fig. 11 reveals the situation with thermal radiation. The surface temperature of the optical windows dropped to approximately 260 K, whereas the hood nose and the surrounding area, which had no cooling jets, declined to approximately 1100 K. The simulation results when adding thermal radiation indicate that this model is better able to conform to the aerothermal conditions of actual flow fields because of the addition of heat flux dissipation.

Fig. 12 shows the optical side window surface temperature distribution at different turbulences and with no thermal radiation. Without radiation, the side window surface temperatures of different turbulence simulations were all approximately 280 K. With radiation, the side window surface temperatures were approximately 260 to 270 K. The temperatures at the ends of the side windows all rose, a result of weaker coverage from the cooling jets, as shown in Figs. 13 and 14. In addition, the surface temperatures of the optical windows were all less than 500 K. If thermal radiation is considered, the amount of cooling jets could be reduced to decrease the missile payload.

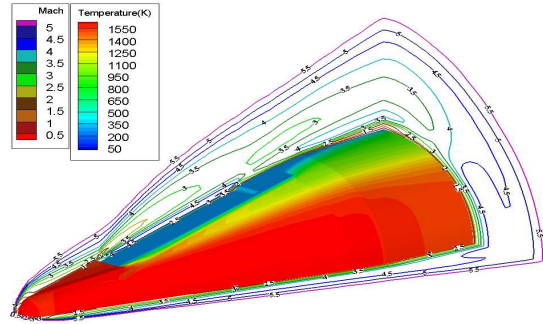


Fig. 10 Mach and temperature contour of model A\_1

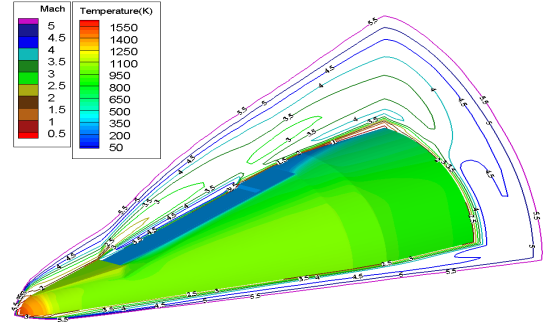


Fig. 11 Mach and temperature contour of model A\_2

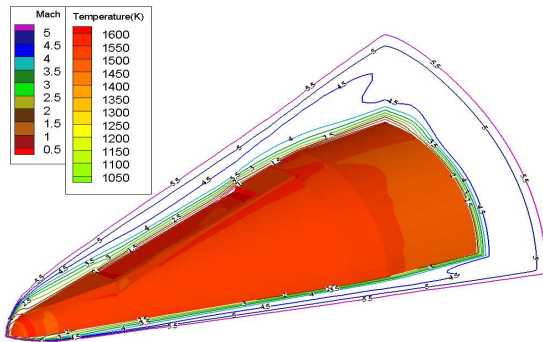


Fig. 8 Mach and temperature contour of model A\_0

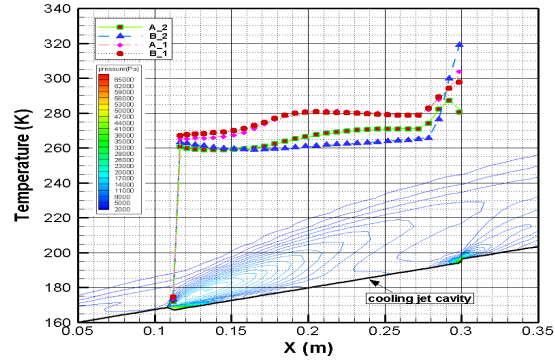


Fig. 12 Surface temperature of optical window in model A\_12, B\_12

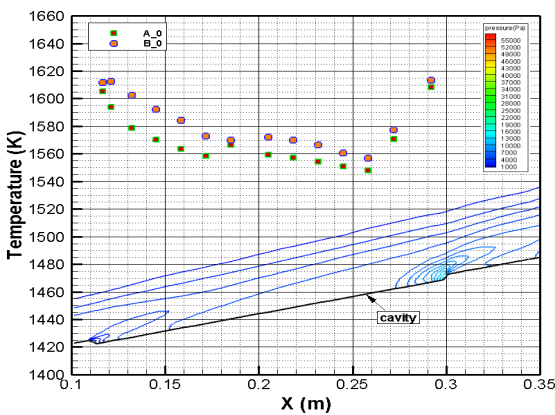


Fig. 9 Surface temperature of optical window in model A\_0, B\_0

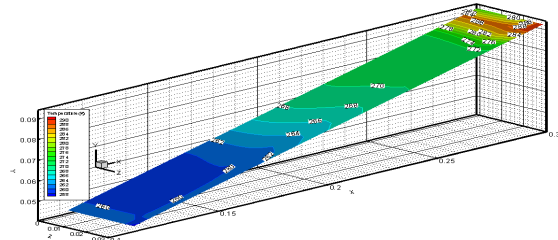


Fig. 13 Surface temperature of optical window in model A\_2

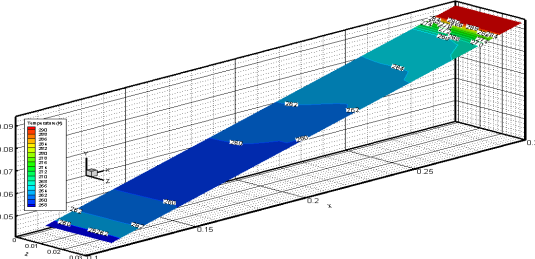


Fig. 14 Surface temperature of optical window in model B\_2

ACKNOWLEDGMENT

The author would like to thank the National Science Council of the Republic of China for financially supporting this research under Contract No. NSC 100-2221-E-606-015.

REFERENCES

- [1] X. Y. Yang, C. H. Liu, and Y. Q. Gu, "Design of hypersonic vehicle infrared cooling dome," *Infrared and Laser Engineering*, vol. 33, no. 6, pp. 576-579, Dec. 2004.
- [2] C. C. Li, Y. C. Lin and, M. C. Hsieh, "3-D simulation of external cooling of aero-optical side window," in *2011 FDIT*. pp. 214-218.
- [3] J. J. Bertin, and R. M. Cummings, " Fifty years of hypersonics: where we've been, where we're going," *Progress in Aerospace Sciences*, vol.39, pp.511-536, 2003.
- [4] K. H. Neale, and, B. M. L. "Active cooling from the sixties to NASP," In: *Current technology for thermal protection systems,* NASA CP 3157, 1992.
- [5] E. H. Hirschel, *Basic of Aerodynamic*, Springer-Verlag, 2005.
- [6] J. Bartl, and M. Baranek, " Emissivity of aluminium and its important for radiometric measurement," *Measurement of Physical Quantities*, vol. 4, pp.31-36, 2004.
- [7] E. R. Dobrovinskaya, L. A. Lytvynov, and V. Pishchik, *Sapphire :Material, Manufacturing, Applications*, Springer-Verlag, 2009, pp.80-95.
- [8] M. Algacyr. Jr., and C. Ndaona, "Hypersonic flow past open cavities," *AIAA Journal*, vol.32, issue.12, pp.2387-2393, 1994.